Understanding Brain Dynamics Through Neural Koopman Operator with Structure-Function Coupling

Chiyuen Chow[1], Tingting Dan[1], Martin Styner[1,2], and Guorong Wu[1,2(✉)]

[1] Department of Psychiatry, University of North Carolina at Chapel Hill, Chapel Hill, USA
grwu@med.unc.edu

[2] Department of Computer Science, University of North Carolina at Chapel Hill, Chapel Hill, USA

Abstract. The fundamental question in neuroscience is to understand the working mechanism of how anatomical structure supports brain function and how remarkable functional fluctuations emerge ubiquitous behaviors. We formulate this inverse problem in the realm of system identification, where we use a geometric scattering transform (GST) to model the structure-function coupling and a neural Koopman operator to uncover dynamic mechanism of the underlying complex system. First, GST is used to construct a collection of measurements by projecting the proxy signal of brain activity into a neural manifold constrained by the geometry of wiring patterns in the brain. Then, we seek to find a Koopman operator to elucidate the complex relationship between partial observations and behavior outcomes with a relatively simpler linear mapping, which allows us to understand functional dynamics in the cliché of control system. Furthermore, we integrate GST and Koopman operator into an end-to-end deep neural network, yielding an explainable model for brain dynamics with a mathematical guarantee. Through rigorous experiments conducted on the Human Connectome Project-Aging (HCP-A) dataset, our method demonstrates state-of-the-art performance in cognitive task classification, surpassing existing benchmarks. More importantly, our method shows great potential in uncovering novel insights of brain dynamics using machine learning approach.

Keywords: Functional-structural Coupling · Neural Koopman Operator · Brain Dynamics.

1 Introduction

The dynamics of the human brain are complex and nonlinear due to the intricate interactions and behaviors of its highly connected structural components [16, 12]. The complexity of brain dynamics is also reflected in the altered spontaneous neuronal activity, which contributes to increased temporal complexity [18]. One

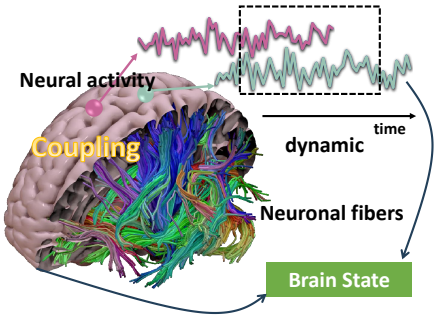

Fig. 1: Our study delves into the coupling mechanism between structural topology and functional dynamic signals (neural activity). By leveraging Koopman Operator theory, we model the brain network as a high-dimensional system, where the Geometric Scattering Transform generates the latent state from observed topology and signals.

of the fundamental science challenges is to understand these complex and nonlinear dynamics by coupling the structural topology information and functional dynamic signals (as shown in Fig. 1).

The brain network representation provides a powerful framework to understand brain dynamics [6, 1, 14]. By coupling the structural connectivity and dynamic signals of each region, we can enhance our understanding of the activity of a brain region in specific states. However, BOLD (blood-oxygenation-level-dependent) signal is an *in-vivo* proxy of brain activity while often accompanied with high level of noisy, which further complicates the already challenging task of understanding the complex brain system. Consequently, conventional linear system representation methods have limited power to capture the patterns of neural activity and dynamics of brain regions.

In this regard, Koopman theory [10] has emerged as a valuable tool for elucidating the underlying dynamics of nonlinear complex systems. This theory enables the representation of nonlinear system dynamics using an infinite-dimensional linear operator, acting on the space of all observable functions of the dynamic system. By linearizing complex brain systems, one can fully characterize them based on their spectral composition. Recent advancements have witnessed the application of deep learning techniques for estimating the Koopman operator. [23, 11, 2].

However, many existing deep learning methods simultaneously learn both the measurement functions and the Koopman operator, often resulting in inaccurate estimations of the Koopman operator. Moreover, the BOLD signal extracted from fMRI, the signal of interest in our study, is inherently unstable and prone to noise from various sources such as instrumental instabilities, head motion, and physiological fluctuations. To address these challenges, we propose a novel data-driven approach called the Scattering Neural Koopman Operator. Our method leverages the Koopman operator framework along with the geometric scattering transform (GST) [7], which is proven to be stable with small perturbations of both signals and structural topology. The GST is used to construct a collection of measurements by projecting the proxy signal of brain activity into a neural manifold constrained by the geometry of wiring patterns in the brain. This in-

novative method aims to enhance Koopman operator estimation accuracy and robustness while effectively handling inherent noise and instability in fMRI data.

Although Koopman operator framework has demonstrated promise in capturing the overarching dynamics embedded within brain network systems, its global and linearized nature may oversimplify the complex, nonlinear dynamics inherent in neurocognitive processes, potentially overlooking the fine-grained, transient patterns of neural activity. To this end, we propose a state control module designed to complement the Koopman operator, which takes BOLD signals as input and generates corresponding control outputs, enabling us to capture and predict the nuanced dynamics of brain activity. Our contributions are three-fold:

- We propose a method named Scattering Neural Koopman Operator which leverages Koopman operator theory and geometric scattering transform to couple structural brain network and brain activity signal to model the global dynamics of the brain system.
- We introduce a control module that can take input to guide the state transition and learn the state-specific activities.
- We conduct experiments on the HCP-A dataset and achieve state-of-the-art performance in cognitive task classification. Further, we delve into the analysis of state-specific brain region activation and investigate how state-specific neurocircuits underline the cognitive functions at various frequencies.

2 Methodology

2.1 Koopman Operator Theory

A sequence of whole-brain BOLD signal $\mathbf{X}_t = \{\mathbf{x}_{t+m}\}_{m=0}^{M-1}$ from time t to $t+M-1$ can be considered as observations of brain states. The nonlinear dynamic brain system can be partially formulated as $\mathbf{x}_{t+1} = \mathbf{F}(\mathbf{x}_t)$, where again $\mathbf{x}_t \in \mathcal{X} \subseteq \mathbb{R}^N$ is the brain system state and $\mathbf{F}(\cdot)$ is a non-linear function expressing the state transition. Considering the complexity of studying nonlinear systems, the Koopman operator theory[10] has been widely used, which can represent a nonlinear dynamic system by an infinite-dimensional linear Koopman operator. Specifically, the linear Koopman operator $\mathcal{K} : \mathcal{G}(\mathcal{X}) \mapsto \mathcal{G}(\mathcal{X})$ acts on a space of measurement functions $\mathcal{G} := \{g : \mathcal{X} \mapsto \mathbb{R}\}$. Then the state transition can be represented by:

$$g(\mathbf{x}_{t+1}) = \mathcal{K}g(\mathbf{x}_t) = g(\mathbf{F}(\mathbf{x}_t)) \tag{1}$$

2.2 Scattering Neural Koopman Operator

Research [13] has confirmed that even with a limited number of measurement functions, an accurate approximation to nonlinear dynamics is achievable if the measurement functions are judiciously selected. Herein, we construct measurements by coupling the structural connectivity and BOLD signals. Specifically,

we utilize geometric scattering transform (GST)[7] to generate multi-scale measurements (as shown in Fig. 2 (a)) because 1) the use of GST aligns closely with the human brain, where we conceptualize that cognition and behavior emerge from spontaneous functional fluctuations supported by neural circuits of physically interconnected brain regions and 2) GST also offers a flexible multi-scale window to elucidate the SC-FC coupling mechanism with great neuroscience insight and mathematical guarantee. We first consider an undirected, weighted and attributed structural brain network $\mathbf{G} = (\mathbf{V}, \mathbf{E}, \mathbf{W})$ with vertices set $\mathbf{V} = \{v_i | i = 1, \ldots, N\}$, an edge set $\mathbf{E} \subseteq \{(v_i, v_j) : 1 \leq i, j \leq N\}$, edge weights $\mathbf{W} = \{w(v_i, v_j) > 0 : (v_i, v_j) \in \mathbf{E}\}$. Then we define the weighted adjacency matrix $\mathbf{A} = [a_{ij}]_{i,j=1}^{N}$ where $a_{ij} = w(v_i, v_j)$ if $(v_i, v_j) \in \mathbf{E}$ and 0 otherwise. Thus the multi-scale graph wavelets $\{\mathbf{\Psi}_h\}_{h=0}^{H-1}$ can be defined as:

$$\begin{aligned} \mathbf{\Psi}_0 &:= \mathbf{I}_N - \mathbf{P}, \quad h = 0 \\ \mathbf{\Psi}_h &:= \mathbf{P}^{2^{h-1}} - \mathbf{P}^{2^h}, \quad 1 \leq h < H \end{aligned} \tag{2}$$

where $\mathbf{I}_N$ is an $N \times N$ identity matrix and $\mathbf{P} = \frac{1}{2}(\mathbf{I}_N + \mathbf{A}\mathbf{D}^{-1})$ is the lazy random walk matrix. Given the wavelet filters, define the one-step propagator with element-wise absolute value function by $\mathbf{U}[h]\mathbf{x}_t := |\mathbf{\Psi}_h|\mathbf{x}_t$. Then the scattering propagator is defined by stacking the one-step propagator (shown in Fig. 2 (b))

$$\mathbf{U}_{p^{(l)}}\mathbf{x}_t := \mathbf{U}[h_l]\mathbf{U}[h_{l-1}], \ldots, \mathbf{U}[h_1]\mathbf{x}_t \tag{3}$$

where $p^{(l)} = (h_1, \ldots, h_l)$ is path (tuple) with $0 \leq h_1, \ldots, h_l < H$ and $|p| = l$. The windowed scattering transform is finally constructed by applying the low-pass filter $\mathbf{\Phi} = \mathbf{P}^{2^H}$ to $\mathbf{U}_{p^{(l)}}\mathbf{x}_t$

$$\mathbf{S}_{p^{(l)}}\mathbf{x}_t := \mathbf{\Phi}\mathbf{U}_{p^{(l)}}\mathbf{x}_t \tag{4}$$

The geometric scattering transform forwards as a tree with each layer consisting of graph-wavelets filters, absolute value function, and a low-pass filter where the input of root node is $\mathbf{X}_t = \{\mathbf{x}_{t+m}\}_{m=0}^{M-1}$. Finally, we stack all these geometric scattering coefficients (tree nodes) to form the multi-scale measurements $\mathbf{Z}_t = \{\mathbf{S}_{p^{(l)}}\mathbf{X}_t | p^{(l)} \in \mathcal{P}^{(l)}, l = 0, 1, \ldots, L\} \in \mathbb{R}^{NB \times M}$, where $\mathcal{P}^{(l)}$ is the set of paths with length l, L is the depth of geometric scattering transform and $B = \sum_{l=0}^{L} H^l$ is the number of GST coefficients. By shifting $\mathbf{X}_t$ one time point forward, we can obtain the paired multi-scale measurements $\mathbf{Z}_{t+1} \in \mathbb{R}^{NB \times M}$. Then the Koopman is estimated by $\mathbf{Z}_t$ and $\mathbf{Z}_{t+1}$. Traditionally, the Koopman operator is calculated by extending Dynamic Mode Decomposition (eDMD)[21] which involves the time-consuming spectral decomposition for each subject (sample). Therefore we utilize trainable matrix $\mathbf{K} \in \mathbb{R}^{NB \times NB}$ to learn the Koopman operator (as shown in Fig. 2 (b)).

2.3 Predict State Transitions with Control

The derived Koopman operator effectively encapsulates the global dynamics inherent in the brain network system. Nonetheless, it is crucial to acknowledge

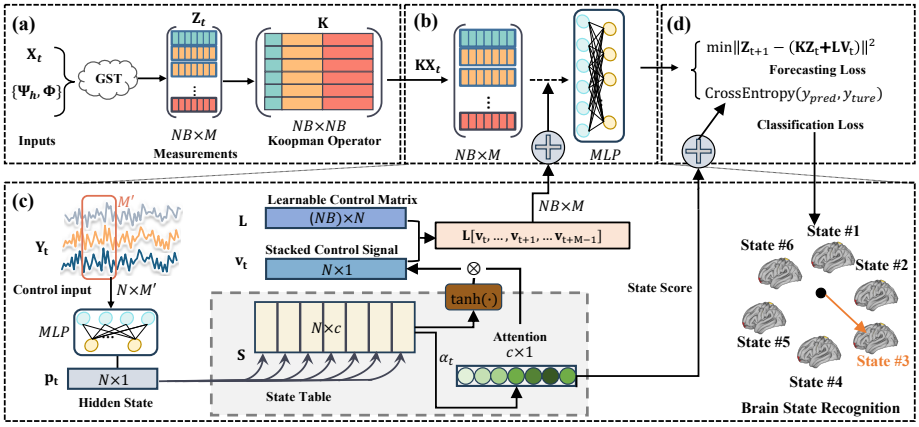

Fig. 2: (a) Measurements and Koopman matrix construction. (b) One-step forward. (c) Control Module. (d) Loss function.

that brain states exhibit rapid variations over short time intervals, which the macroscopic perspective of the Koopman operator may fail to adequately capture. Therefore, we introduce control input $\mathbf{Y}_t$ for each time point $\mathbf{z}_t$ to guide the dynamics forward to the desired brain state. Here the control input $\mathbf{Y}_t$ we use is also the BOLD signal sequence like $\mathbf{X}_t$ but with a much smaller window size. Specifically, given a sequence of control input $\mathbf{Y}_t \in \mathbb{R}^{N\times M'}$, where M' is the length of the input frame, we first feed $\mathbf{Y}_t$ to an encoder ϕ and transform along the temporal dimension to get a hidden state $\mathbf{p}_t = \phi(\mathbf{Y}_t) \in \mathbb{R}^N$. This hidden state $\mathbf{p}_t$ thus contains information about the input frame $\mathbf{Y}_t$. Moreover, we define a learnable state table $\mathbf{S} \in \mathbb{R}^{N\times C}$ where C is the number of states and each $\mathbf{S}_i, \forall i = 0, \ldots, C-1$ corresponds to one specific brain state (shaded in Fig. 2 (c)). Next, we generate the control signal at time t by measuring how hidden state $\mathbf{p}_t$ matches the states in $\mathbf{S}$ and then weighted summation:

$$\mathbf{v}_t = \sum_{i=0}^{C-1} \alpha_t^i tanh(\mathbf{S}_i) \in \mathbb{R}^N \tag{5}$$

where $\alpha_t = \text{SoftMax}\left((\mathbf{W}_Q\mathbf{p}_t)^\top(\mathbf{W}_K\mathbf{S})\right) \in \mathbb{R}^C$ is the attention weight. Hence, the control signal $\mathbf{v}_t$ is the weighted sum of brain states in state table. We further cascade $\{\mathbf{v}_{t+m}\}_{m=0}^{M-1}$ from time t to $t+M-1$ to form a matrix $\mathbf{V}_t$ which matches the size of $\mathbf{Z}_t$ in temporal dimension. Finally, to train the model, we define the following losses. The first one is the Koopman loss:

$$\mathcal{L}_{Koop} = \frac{1}{M}\left\|\mathbf{Z}_{t+1} - \mathbf{K}\mathbf{Z}_t - \mathbf{L}\mathbf{V}_t\right\| \tag{6}$$

where $\mathbf{L} \in \mathbb{R}^{NB \times N}$ is the learnable control matrix for generating control output measurements. Then the classification loss is calculated as follows:

$$\mathbf{y}_{pred} = \frac{1}{M}(\phi_1(\mathbf{K}\mathbf{Z}_t + \mathbf{L}\mathbf{V}_t))\mathbf{1} + \frac{1}{M}\sum_{m=0}^{M-1}\alpha_{t+m} \tag{7}$$

$$\mathcal{L}_{cls} = \text{CrossEntropy}(\mathbf{y}_{pred}, \mathbf{y}_{true}) \tag{8}$$

where Eq. 7 means that the classification logits depend on both the evolved measurements and the attention score. In Eq. 7, ϕ_1 transform the dimension of measurements from NB to C and $\mathbf{1} \in \mathbb{R}^M$ is an all-one column vector that sums up the results along time dimension. This mean-pooling in time-dimension can utilize the information of the whole sequence. Together, the total loss function $\mathcal{L}$ can be represented by (Fig. 2 (d))

$$\mathcal{L} = \beta\mathcal{L}_{Koop} + (1-\beta)\mathcal{L}_{cls} \tag{9}$$

where β is the hyperparameter for balancing the Koopman loss and identification loss. We name our method as SKoop-C, which stands for Scattering Neural Koopman Operator with Control. An overview of SKoop-C is shown in Fig. 2.

3 Experiments

3.1 Dataset and Experimental Setup

All experiments were conducted using data recruited from the Human Connectome Project - Aging (HCP-A) dataset [5]. HCP-A includes data from 717 subjects, encompassing both fMRI (4,846 time series) and Diffusion Weighted Imaging (DWI) (717) scans. This rich collection facilitates in-depth analyses of both functional and structural connectivity. The HCP-A dataset includes data from four brain tasks associated with memory: VISMOTOR, CARIT, FACENAME, and Resting State. Each fMRI scan consists of 125 time points. In the following experiments, these tasks are treated as distinct categories in a four-class classification problem. We partition each into 90 regions using AAL atlas [19]. Thus, SC is a 90×90 matrix where each element is quantified by the number of fibers linking two brain regions.

We compare SKoop-C with a variety of current state-of-the-art methods. (1) *GNN variants.* We consider Graph Attention Networks (GAT) [20], Graph Isomorphism Network(GIN) [22], and the general, powerful, scalable graph transformer (GPS) [15]. (2) *Transformer variants.* BolT [4] ,which is a transformer specially designed for BOLD-signal-related tasks. (3) *Time-series-related methods.* We consider Long Short-Term Memory (LSTM) [9] and Temporal Convolutional Network (TCN) [3], which both are designed for time-series tasks. The evaluation metrics include accuracy (Acc.), precision (Prec.), recall (Rec.), and F1 score (F1.). The dataset is divided into train/validation/test sets as $6:1:3$.

Table 1: Performance of competing methods and our SKoop-C in recognizing four cognitive tasks from functional neuroimages in HCP-A.

Methods	GIN	GAT	GPS	TCN	LSTM	BolT	SKoop	KAE	KAE-C	SKoop-C
Acc.(%)	41.91	81.22	76.59	84.27	70.15	92.07	85.36	63.78	87.93	**94.12**
Prec.(%)	41.52	81.31	76.67	84.44	70.35	92.16	85.49	64.20	88.08	**94.32**
Rec.(%)	41.71	81.83	76.91	84.24	70.35	92.14	85.71	66.35	88.08	**94.85**
F1.(%)	41.48	81.30	76.77	84.28	70.30	92.10	85.50	63.46	88.07	**94.56**

3.2 Recognition of Cognitive Tasks on HCP-A

In this sequence of experiments conducted on the HCP-A dataset, we explore task-specific recognition by employing an array of methods, namely GIN, GAT, GPS, TCN, LSTM, BolT, and our SKoop-C model. Table 1 (left) lists the experimental results. The outcomes distinctly highlight the superior performance of our approach, in contrast to other methods which exhibited a decline in effectiveness. GIN, GAT, and GPS represent the category of message-passing methods. Their inputs are the structural connectivity and functional connectivity with 0.5 thresholding instead of the raw BOLD signals for better performance. GIN, although theoretically profound, has shown limited effectiveness in this context, achieving an accuracy of 41.91%, while the other two GNN variants achieve significantly better performance thanks to the attention mechanism. An obvious contrast in performance is observed with the introduction of time-series-related methods like TCN and BolT. These methods are designed to learn temporal features, which is a critical advantage over the previously discussed message-passing methods. Note that their inputs are raw BOLD signals different from the previous GNN-models. While our SKoop-C uses geometric scattering transform with structural connectivity and raw BOLD signals as input, which has proven to be stable to perturbations on graphs and signals. This stability is crucial in maintaining the integrity of the extracted features amidst the complexities of cognitive tasks. The Koopman theory and control module also extend our model's capability to unravel the intricate dynamics of the system as well as the ability to retain and recall state-specific information, enhancing the model's contextual awareness. The result underscores the power of our methodology in handling complex cognitive tasks.

3.3 Ablation Studies

We also conducted ablation experiments on our methods to comprehensively verify the influence of different modules. Table 1 (right) indicates the experiment results, where KAE is implemented using Koopman operator with measurements learnt by auto encoder, SKoop is Scattering Neural Koopman operator without control module and KAE-C is KAE with control. The introduction of the Scattering Neural Koopman Operator (SKoop) without the control module marks

a significant improvement over KAE. This suggests that the addition of geometric scattering helps in better capturing the intrinsic geometrical features of the brain's structural connectivity and its dynamic signals, leading to improved metrics compared to KAE. And the addition of the state control module to KAE (marked as KAE-C) results in a notable improvement across all metrics. This indicates that incorporating control inputs into the Koopman framework allows for more precise modeling and prediction of brain dynamics. Finally, SKoop-C, which combines the Scattering Neural Koopman Operator with a control module, achieves the highest performance across all metrics. The control module's ability to guide state transitions and the geometric scattering's robust feature extraction capabilities evidently provide a principled framework for accurately classifying cognitive tasks.

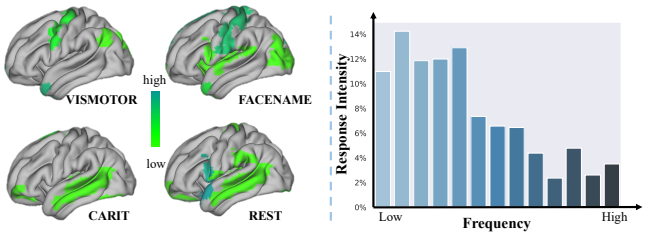

Fig. 3: Left: Critical brain regions (top-8) linked to four tasks are depicted. Right: The histogram of wavelet frequencies in the control matrix.

3.4 Interpretation from Control Module

In this section, we utilize the control signal of each state ($tanh(\mathbf{S}_i)$ in Eq. 5) to show that our method can provide interpretable visualization of activate regions in different task states. Specifically, we select the top eight regions for each state that manifest the largest absolute values. Fig. 3 (left) presents the brain mapping of the selected top 8 regions of each cognitive tasks. For instance, the selected task-specific regions in VISMOTOR task are mostly located in the somatosensory and motor cortex, which is closely aligned with current neuroscience findings [8]. In addition, we also investigate the frequency characteristics of the control response when given input of each region. According to the definition of the control matrix $\mathbf{L}$ in Eq. 6, it shows how a region signal in a specific frequency will respond to an input. We therefore display the histogram of wavelet frequencies in the control matrix in Fig. 3 (right). We observed that the energy of control is distributed extensively in the low-frequency band, while relatively sparse in the high-frequency band. Although the examination brain stimulation and cognitive control [17] is beyond the scope of this paper, the output of our method offers a new window to understand the complex dynamical system of human brain using explainable meachine learning approaches.

4 Conclusion

In conclusion, our research introduced a streamlined method for analyzing brain dynamics, the Scattering Neural Koopman Operator with Control, utilizing the power of Koopman operator theory and geometric scattering transform. Our experiments on HCP-A datasets highlighted the method's efficacy in accurately capturing and predicting complex brain activities, surpassing current benchmarks. The findings from our detailed analysis underscore our approach's robustness against the inherent noise in BOLD signals and reveal insightful patterns of brain region activation and their responses across different cognitive tasks. In the future, we will focus on the scalablity in estimating Koopman operator, which is computationally expensive to estimate Koopman operator as more and more brain regions are taken into account. The possible solution is to introduce additional constraints to make it scale up to a fine-grained atlas or even a voxel-based manner.

Disclosure of Interests. The authors have no competing interests to declare.

References

1. Abdelnour, F., Voss, H.U., Raj, A.: Network diffusion accurately models the relationship between structural and functional brain connectivity networks. Neuroimage **90**, 335–347 (2014)
2. Azencot, O., Erichson, N.B., Lin, V., Mahoney, M.: Forecasting sequential data using consistent koopman autoencoders. In: International Conference on Machine Learning. pp. 475–485. PMLR (2020)
3. Bai, S., Kolter, J.Z., Koltun, V.: An empirical evaluation of generic convolutional and recurrent networks for sequence modeling. arXiv preprint arXiv:1803.01271 (2018)
4. Bedel, H.A., Sivgin, I., Dalmaz, O., Dar, S.U., Çukur, T.: Bolt: Fused window transformers for fmri time series analysis. Medical Image Analysis **88**, 102841 (2023)
5. Bookheimer, S.Y., Salat, D.H., Terpstra, M., Ances, B.M., Barch, D.M., Buckner, R.L., Burgess, G.C., Curtiss, S.W., Diaz-Santos, M., Elam, J.S., et al.: The lifespan human connectome project in aging: an overview. Neuroimage **185**, 335–348 (2019)
6. Galán, R.F.: On how network architecture determines the dominant patterns of spontaneous neural activity. PloS one **3**(5), e2148 (2008)
7. Gao, F., Wolf, G., Hirn, M.: Geometric scattering for graph data analysis. In: International Conference on Machine Learning. pp. 2122–2131. PMLR (2019)
8. Glasser, M.F., Sotiropoulos, S.N., Wilson, J.A., Coalson, T.S., Fischl, B., Andersson, J.L., Xu, J., Jbabdi, S., Webster, M., Polimeni, J.R., et al.: The minimal preprocessing pipelines for the human connectome project. Neuroimage **80**, 105–124 (2013)
9. Hochreiter, S., Schmidhuber, J.: Long short-term memory. Neural computation **9**(8), 1735–1780 (1997)
10. Koopman, B.O.: Hamiltonian systems and transformation in hilbert space. Proceedings of the National Academy of Sciences **17**(5), 315–318 (1931)
11. Li, Y., He, H., Wu, J., Katabi, D., Torralba, A.: Learning compositional koopman operators for model-based control. arXiv preprint arXiv:1910.08264 (2019)

12. Mayer-Kress, G.: Non-linear mechanisms in the brain. Zeitschrift für Naturforschung C **53**(7-8), 677–685 (1998)
13. Nathan Kutz, J., Proctor, J.L., Brunton, S.L.: Applied koopman theory for partial differential equations and data-driven modeling of spatio-temporal systems. Complexity **2018**, 1–16 (2018)
14. Raj, A., Kuceyeski, A., Weiner, M.: A network diffusion model of disease progression in dementia. Neuron **73**(6), 1204–1215 (2012)
15. Rampášek, L., Galkin, M., Dwivedi, V.P., Luu, A.T., Wolf, G., Beaini, D.: Recipe for a general, powerful, scalable graph transformer. Advances in Neural Information Processing Systems **35**, 14501–14515 (2022)
16. Shettigar, N., Yang, C.L., Tu, K.C., Suh, C.S.: On the biophysical complexity of brain dynamics: An outlook. Dynamics **2**(2), 114–148 (2022). https://doi.org/10.3390/dynamics2020006, https://www.mdpi.com/2673-8716/2/2/6
17. Smith, J., Johnson, E.: Cognitive control mechanisms in developmental disorders: From robots to humans. Journal of Cognitive Neuroscience **29**(4), 567–580 (2017)
18. Sporns, O.: The complex brain: Connectivity, dynamics, information. Trends in Cognitive Sciences **26**(12), 1066–1067 (2022)
19. Tzourio-Mazoyer, N., Landeau, B., Papathanassiou, D., Crivello, F., Etard, O., Delcroix, N., Mazoyer, B., Joliot, M.: Automated anatomical labeling of activations in spm using a macroscopic anatomical parcellation of the mni mri single-subject brain. Neuroimage **15**(1), 273–289 (2002)
20. Veličković, P., Cucurull, G., Casanova, A., Romero, A., Lio, P., Bengio, Y.: Graph attention networks. arXiv preprint arXiv:1710.10903 (2017)
21. Williams, M.O., Kevrekidis, I.G., Rowley, C.W.: A data-driven approximation of the koopman operator: Extending dynamic mode decomposition. J. Nonlinear Sci. **25**(6), 1307–1346 (2015). https://doi.org/10.1007/S00332-015-9258-5, https://doi.org/10.1007/s00332-015-9258-5
22. Xu, K., Hu, W., Leskovec, J., Jegelka, S.: How powerful are graph neural networks? arXiv preprint arXiv:1810.00826 (2018)
23. Yeung, E., Kundu, S., Hodas, N.: Learning deep neural network representations for koopman operators of nonlinear dynamical systems. In: 2019 American Control Conference (ACC). pp. 4832–4839. IEEE (2019)